4.3 THE EFFECT OF FRICTION AND GRAVITY

As mentioned previously, one of the major goals of a robot is to move a tool or a part from one point to another in an accurate and repeatable manner. Anything that prevents this goal from being achieved is clearly undesirable and must, therefore, either be compensated for or eliminated. In practically all electromechanical, pneumatic–mechanical, or hydraulic–mechanical systems, friction in various components will create a position error. Also, gravity will produce a position error of varying magnitude in one or more joints for most robots. To see more clearly the effects of these "disturbances," it will be necessary first to consider a more complete model of a dc servomotor.

4.3.1 Modeling the DC Servomotor

One of the common methods of driving a robotic joint is through the use of a dc servomotor, a fractional-horsepower motor with a stationary magnetic field that is generated by a permanent magnet. [For this reason it is sometimes called a permanent-magnet (PM) motor.] No power is used in the stator structure of this device and the field is constant over a wide range of armature currents. A PM motor usually requires less cooling than do other types of dc motors (e.g., a shunt motor). Other advantages of the PM motor over the wound types are:

1. High stall torque. This is an important characteristic during joint acceleration and also when the manipulator is required to keep a load stationary.
2. Smaller frame size and lighter weight for a given output power. This is especially important in a robot, where the design may require the motor to be moved within the joint itself.
3. The speed–torque curve of a PM motor is linear, as shown in Figure 4.3.1. If these curves were nonlinear, a potentially significant amount of extra computational effort might be required of the joint processor to ensure that a given amount of torque (or current) was produced by the motor.

A linear circuit model of a dc servomotor armature is shown in Figure 4.3.2. Here R_a is the total armature resistance (including that due to the brushes), R_L is a resistance that represents the magnetic losses in the armature (and is normally $>> R_a$ since these losses are usually small at the frequencies of interest), L_a is the armature inductance, and E_g is the back EMF produced when the armature rotates in a dc magnetic field. This last term is proportional to the angular velocity $\omega(t)$ of the armature (i.e., $\dot{\theta}$). That is,

$$E_g = \omega(t)K_E \tag{4.3.1}$$

where K_E is referred to as the back EMF constant of the motor. Applying ele-

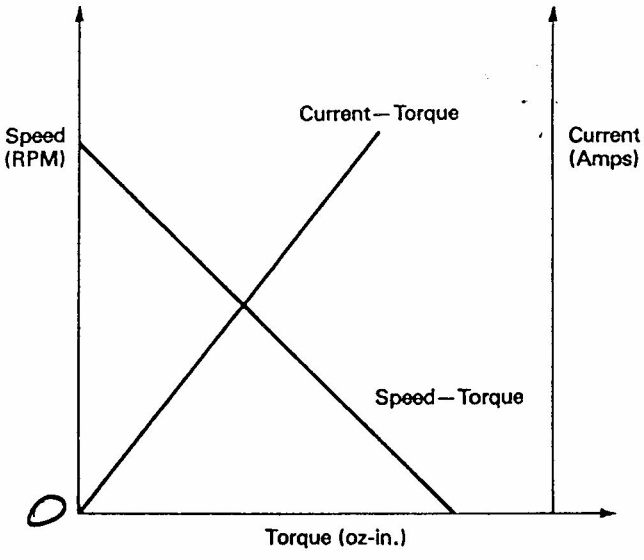

Figure 4.3.1. Speed and current versus torque for a DC servomotor.

mentary circuit theory to Figure 4.3.2 and using Eq. (4.3.1) gives

$$V_{arm} = R_a I_a + L_a \dot{I}_a + \omega(t) K_E \tag{4.3.2}$$

I_a and $\dot{I}_a$ represent the armature current and its time derivative.

As shown in Eq. (4.3.1) and Fig. (4.3.1) the torque generated by the armature moving in a PM field is linearly related to the current. Thus

$$T_g = K_T I_a \tag{4.3.3}$$

where K_T is the torque constant. This generated torque is required to accelerate an inertia (usually consisting of the motor armature itself and an external load), overcome any viscous damping torque due to the motion of the armature, and to

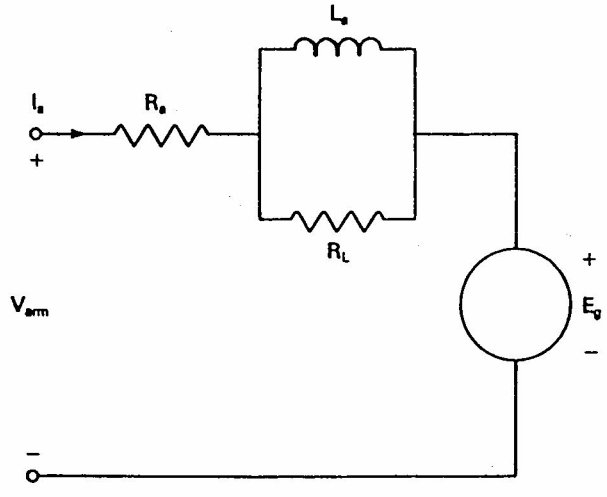

Figure 4.3.2. Circuit model of a DC servomotor armature.

overcome any external load torque (e.g., due to either gravity or static friction). Thus we may write

$$T_g = (J_M + J_L)\,\dot{\omega}(t) + B\omega(t) + T_f + T_{gr} \tag{4.3.4}$$

In this equation, J_M and J_L are the armature and reflected load inertias (which for convenience will be combined and written as $J_T = J_M + J_L$), B is the armature viscous damping coefficient, T_f is the friction torque of the motor and the load (including the gears, etc.), and T_{gr} is the gravitational torque load. This model assumes that all components of the rotary system turn in phase (i.e., there is no torsional resonance in the system; this topic is discussed in Section 3.5.3.1). Note that if the load has any viscous friction, this can be added to B.

Combining Eqs. (4.3.1) through (4.3.4), the model of a servomotor (including the friction and gravity terms) is found to be the one shown in Figure 4.3.3. Using block diagram reduction techniques, the transfer function of the motor becomes

$$G_m(s) = \frac{\Omega(s)}{V_{\text{arm}}(s)}$$

$$= \frac{K_T/L_aJ_T}{s^2 + [(R_aJ_T + L_aB)/L_aJ_T]s + (K_TK_E + R_aB)/L_aJ_T} \tag{4.3.5}$$

It is important to note that the disturbance torques T_f and T_{gr} do not appear in this expression because they are treated as additional *inputs*. They will be utilized, however, later in this section.

In developing the results above, it has been assumed that the load inertia (reflected back to the motor shaft) does not vary with time, so that J_L is a constant. This nontrivial assumption is valid for a large number of applications. Unfortunately, however, the actuation of a robotic joint is usually not one of them. In fact, the reflected inertia of most of the axes of a robot will normally fluctuate significantly while the manipulator is moving. An example of such behavior can be seen in Figure 4.3.4, where the inertia variation for each of the six joints of a JPL-Stanford arm is shown. It is observed that the inertia of joint 1 (i.e., the

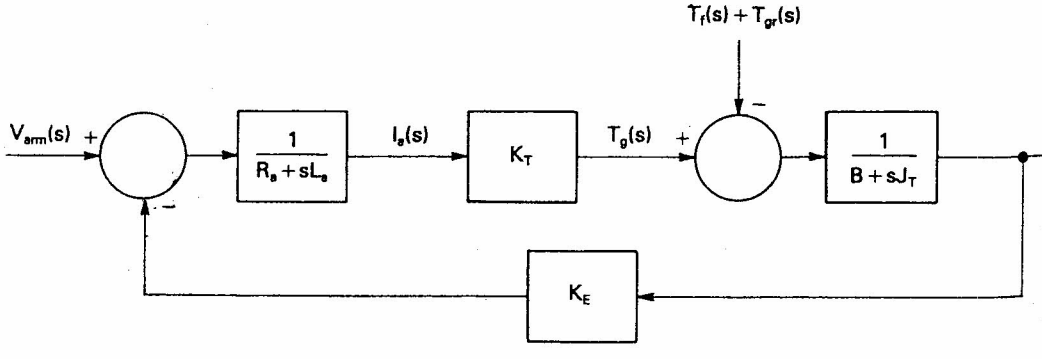

Figure 4.3.3. Block diagram of DC servomotor including gravitational and friction disturbance torques.

MOTOR — see Equation 4.135 p 212

$$\frac{G_{im}}{1 + G_{im}H}$$

MOTOR HAS FEEDBACK K_E!

$$G_m(s) = \frac{K_T}{(R_a + sL_a)} \frac{1}{(B + sJ_m)} \qquad H = K_E$$

$$\frac{G}{1 + GH} = \frac{\frac{K_T}{A \cdot B}}{1 + \frac{K_T}{A \cdot B} \cdot K_E} = \frac{K_T}{A \cdot B + K_T K_E}$$

$$= \frac{K_T}{(R_a + sL_a)(B + sJ_m) + K_T K_E}$$

MOTOR = $G_m(s)$

Should be $G_m(s)$ on p 214 ✓ See MATLAB PROGRAM

$$\frac{7.778 \times 10^5}{s^2 + 4884.027s + 5.526 \times 10^4}$$

$$G_m(s) = \frac{K_T}{s^2 L_a J_m + s(L_a B + R_a J_m) + R_a B + K_T K_E}$$

$$= \frac{K_T / L_a J_m}{s^2 + s\left(\frac{L_a B + R_a J_m}{L_a J_m}\right) + \frac{R_a B + K_T K_E}{L_a J_m}}$$

See MATLAB FIG 1 STEP RESPONSE

Rise time ≈ 14 ms Final value ≈ 14

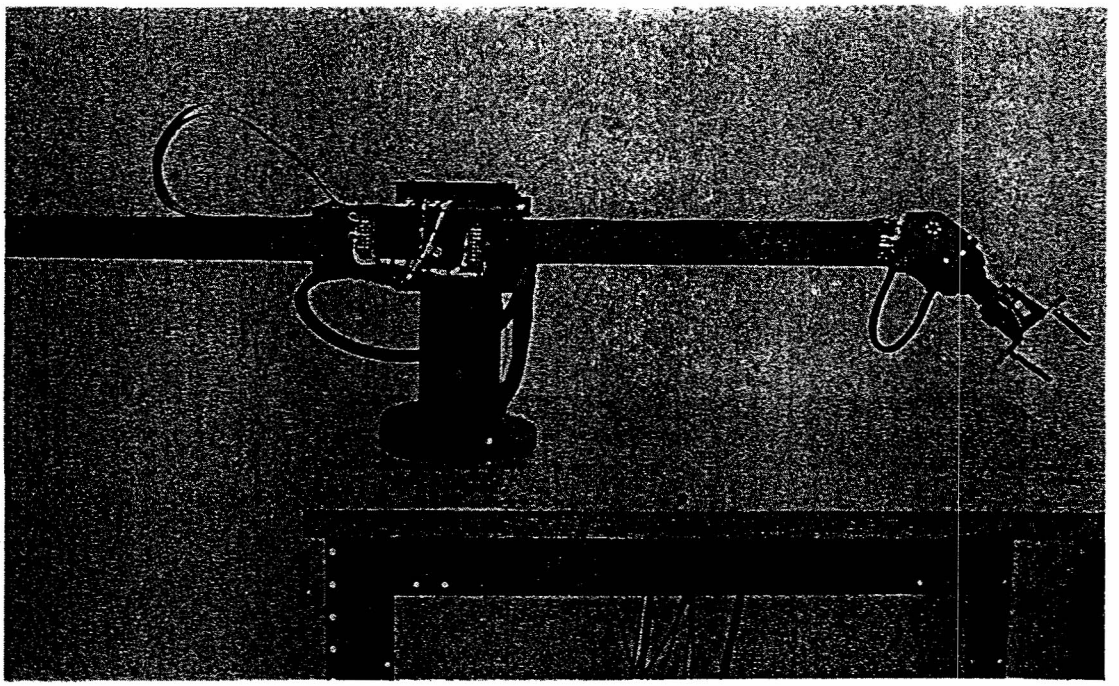

Figure 1.2.2. Jet Propulsion Laboratory—Stanford arm. This 6-axis, electrically actuated robot utilizes the Scheinmann design with JPL modifications. (Courtesy of Dr. A. K. Bejczy and Jet Propulsion Laboratories, Pasadena, CA.)

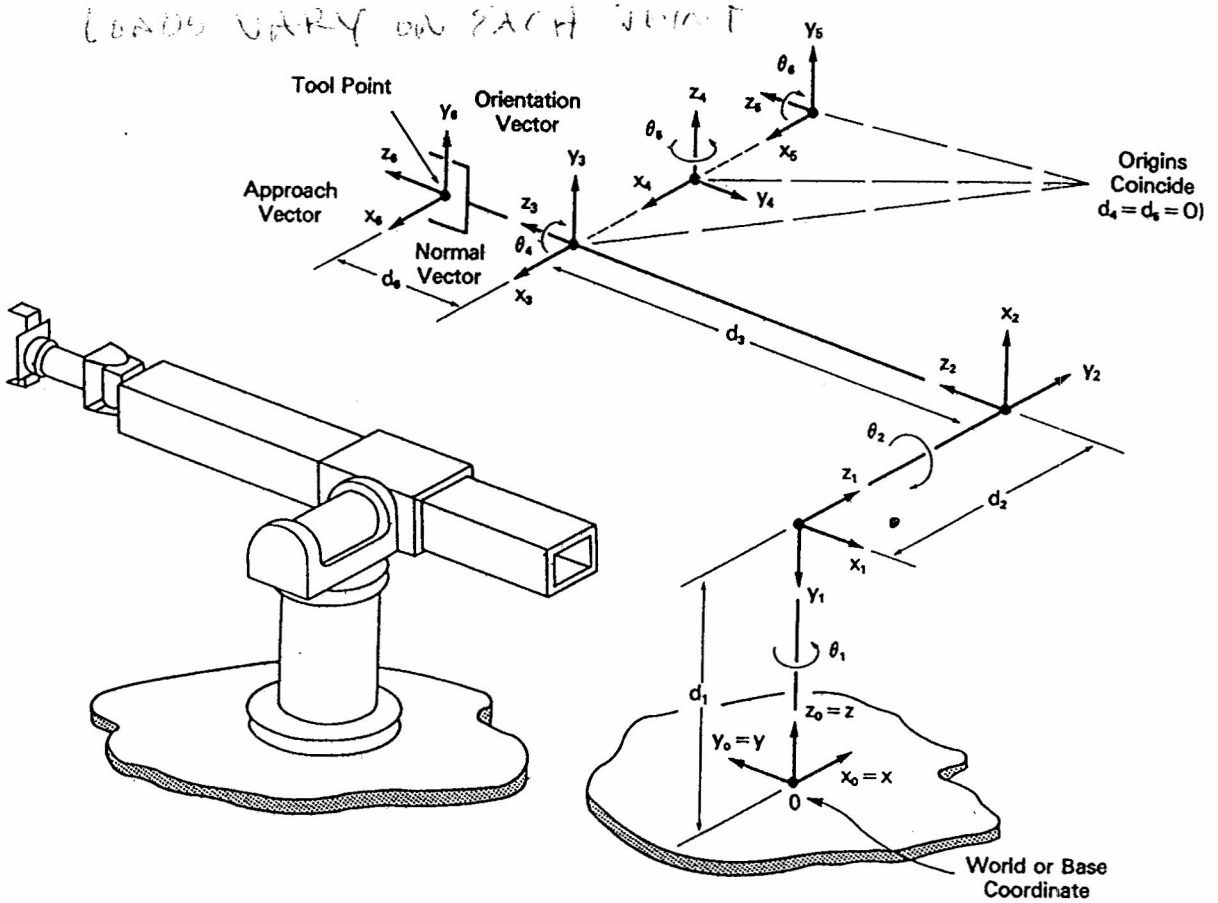

Figure 8.6.7. Coordinate frames for the Stanford arm. (Reproduced with the permission of SRI International, Menlo Park, CA.)

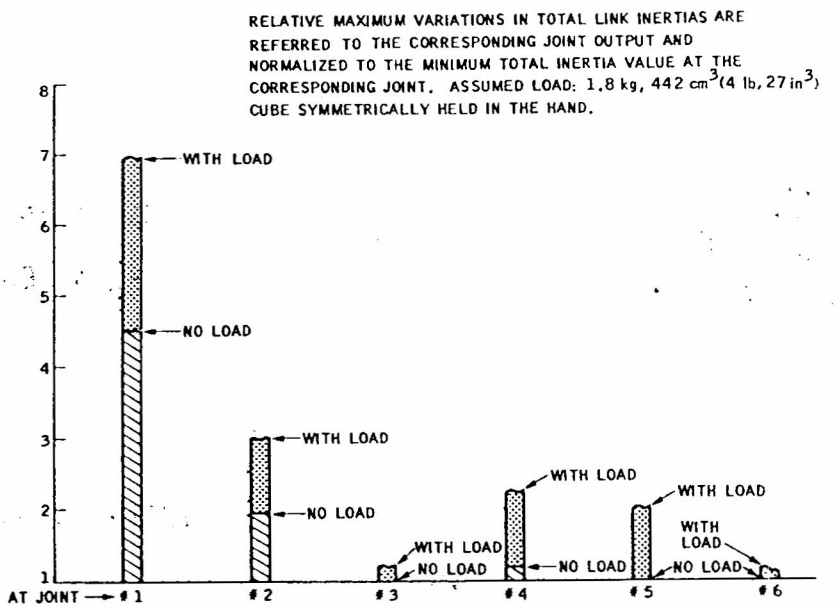

Figure 4.3.4. Inertia variations for each of the six joints of a JPL-Stanford arm. Both variations with and without a load (carried by the gripper) are shown. (Courtesy of A.K. Bejczy and Jet Propulsion Laboratories, Pasadena, CA.)

"trunk") varies approximately 4.5 times under no load conditions and by as much as 7 times when the manipulator is carrying a 4-1b load. Joints 2, 4, and 5 are seen to have significant variations also. Only axes 3 and 6 have relatively constant inertias over their entire range of travel. This behavior is typical of other robots, although the specific inertia fluctuations may be different. Despite the fact that the inertia of a robotic joint usually does undergo dramatic changes as a function of the manipulator position, it is common design and control practice to ignore this and to assume that J_L is a constant. The resultant computational simplification permits a "worst-case" approach to be used whereby the motor and associated mechanical linkages and gears are selected for the maximum load (i.e., inertia) conditions. It is apparent that this may not produce the lowest-cost design. Alternatively, the system is "derated" under full load so that maximum acceleration is not permitted under this condition. Hence, smaller, less costly components may be used.

Regardless of which of these design processes is selected, the control of the individual joints of a robot is usually accomplished by assuming that there is no time variation of the load inertia. Compromises in performance are the inevitable consequence (e.g., reduced speed and/or payload capability of the manipulator). It is reasonable to expect, however, that as microprocessors become more powerful and cost-effective, adaptive schemes that compensate for the large changes in reflected inertia will be used. A corresponding improvement in performance will undoubtedly result. This is discussed briefly in Section 4.5.5.

MATLAB 2/2010

EXAMPLE 4.3.1

Let us find the poles [i.e., the roots of the denominator polynomial of $G_m(s)$] of a commercially available dc servomotor. For example, the parameters of an Electrocraft Corporation E530 motor are:

SEE P719 LIST OF MOTORS APPENDIX B

$K_T = 10.02$ oz-in./A TORQUE CONST.

$K_E = 7.41$ V/1000 rpm BACK EMF

$R_a = 1.64\ \Omega$ (including brush resistance)

$L_a = 3.39$ mH

$B = 0.1$ oz-in./1000 rpm

$J_M = 0.0038$ oz-in.-s^2 ROTOR INERTIA

Assuming that there is no inertial load coupled to the motor shaft, $J_T = J_M$ in Eq. (4.3.5). Since the gravity and friction terms do not affect the motor poles, we may also assume that T_f and T_{gr} are both zero, so that Eq. (4.3.5) is applicable. To utilize this equation, K_E and B first must be converted to V/rad/s and oz-in./rad/s, respectively, in order to have a consistent set of units. This is accomplished by dividing each of the given parameters by 104.72. Thus

1000 rev/min $\times \frac{1\text{min}}{60\text{s}} \cdot \frac{2\pi\text{rad}}{\text{rev}}$ $\simeq 104$ rad/sec

$K_E = 0.0708$ V/rad/s

$B = 9.55 \times 10^{-4}$ oz-in./rad/s

These parameters can now be substituted into Eq. (4.3.5). The actual transfer function for the Electrocraft motor is found to be

NOTE $G_m = \frac{G_{lm}}{1 + G_{lm} \cdot KE}$

G_{lm} = EQ 4.3.5

$$G_m(s) = \frac{7.778 \times 10^5}{s^2 + 484.027s + 5.516 \times 10^4}$$

As mentioned above, the roots of the denominator polynomial will give the motor poles. Thus

$\tau_1 = 34$ ms $s_1 = -183.621$ rad/s $\tau = \frac{2\pi}{\omega}$

$\tau_2 = 20$ ms $s_2 = -300.406$ rad/s

both of which are observed to be negative and real. This is quite often the case for commercial servomotors, implying that the open-loop response of such motors (to a step voltage on the armature) will be, in general, *overdamped*.

The model of the motor used in Figure 4.2.2 can now be replaced by the one just developed in Figure 4.3.3. This is shown in Figure 4.3.5. Using standard

```
% Motor Control Example  Like Klafter Equation 4.3.5 example
%  In this example, define the constants for numerator and denominator
%  G(s)= .06Kp/[s+0.01(1+0.1Kp)]s
clear all, clf, clc
% Different values of the gain
Kp = 100;              % 100
num = .06*Kp;          % Numerator
den = [1 .01+.001*Kp];  % Denominator
help step              % Study the step function
% Look at the G(s) as a transform
sys1=tf(num,den)    % ans =   6/(s + 0.11), could plot step(sys)
t = 0:.4:50;           % Define the time scale
y1 = step(num,den,t);   % This creates the step function but no plot
Kp = 200;              % 200
num = .06*Kp;
den = [1 .01+.001*Kp];
y2 = step(num,den,t);
Kp = 500;
num = .06*Kp;
den = [1 .01+.001*Kp];
%  Do a Plot with three values of Kp
y3 = step(num,den,t);
figure(1)
plot(t,y1,t,y2,t,y3),grid,title('Simple Motor Step functions');
xlabel('Time (sec)'),ylabel('y(t)')
% the following adds a legend
hold on
plot([13 21],[39 37],[9 21],[45 41],[5 21],[52 45]) % Draw the lines
text(22,45,'Kp = 500'),text(22,41,'Kp = 200'),text(22,37,'Kp = 100')
hold off
```

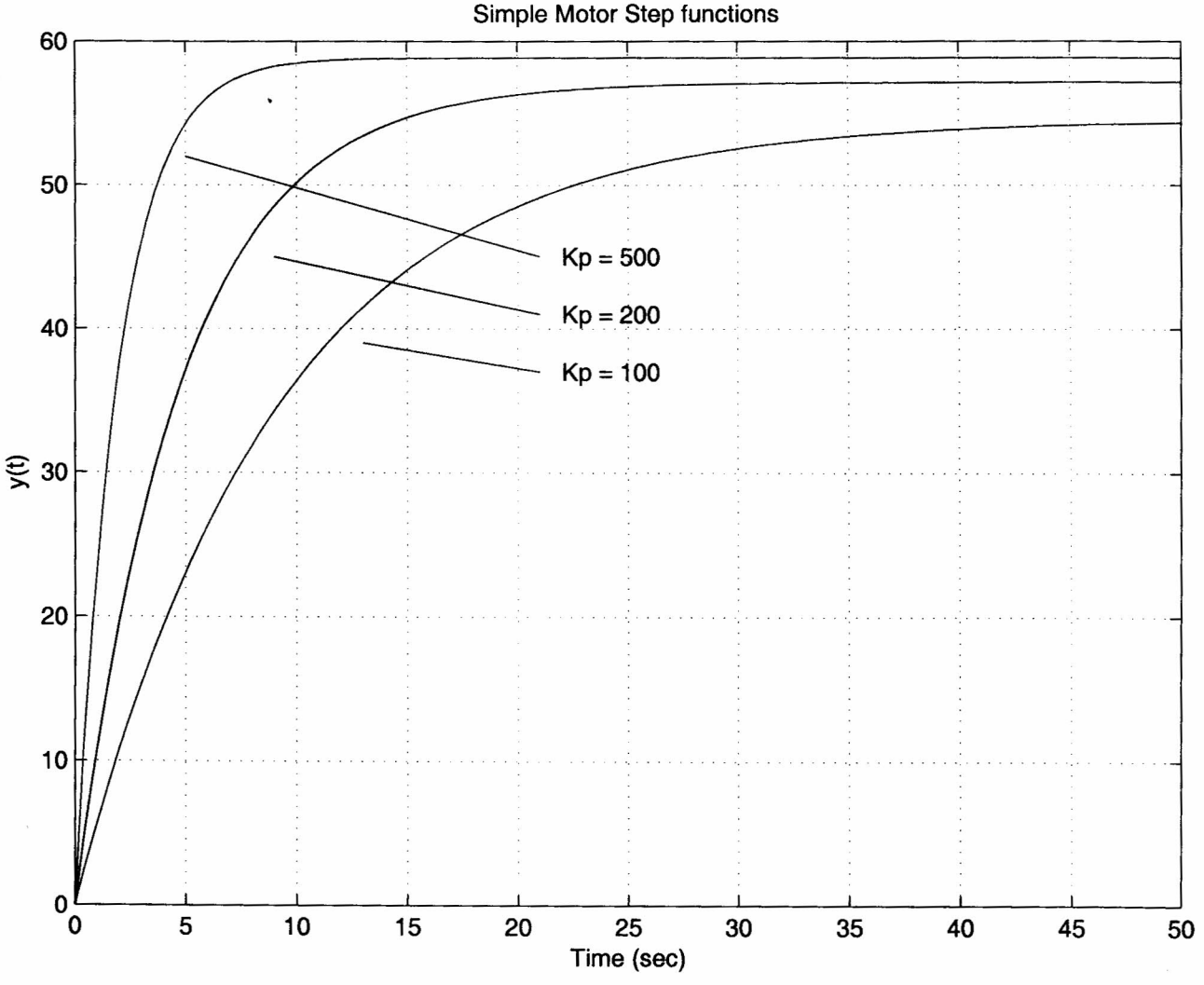
Simple Motor Step functions
60
50
40
30
20
10
0
y(t)
0
5
10
15
20
25
30
35
40
45
50
Time (sec)
Kp = 500
Kp = 200
Kp = 100

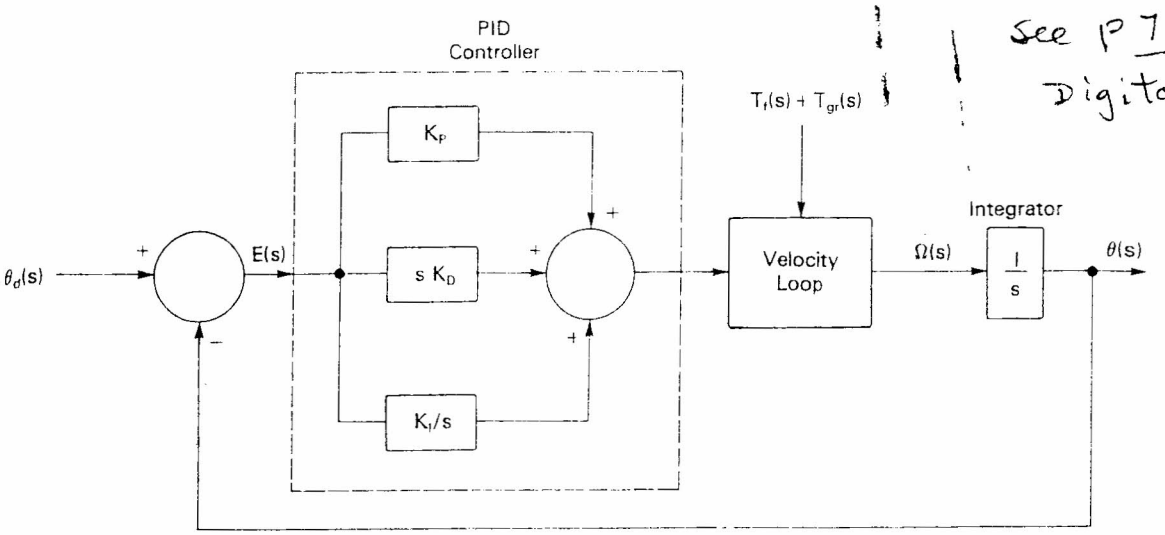

Figure 4.3.6. Position servo with a PID controller.

The minimum value of position gain that will keep the position error due to a torque disturbance below a certain value is seen to be

$$K_{p_{\min}} = \frac{R_a T_L}{A K_T \theta_{\max}} \tag{4.3.11}$$

If the specified value of the hysteresis is small, the value of K_p will be large. In fact, this value may be so large that the joint response will either be unstable or highly underdamped (recall the discussion in Sections 4.2.1 and 4.2.2). Under these circumstances, it will be necessary to use a good deal of tach feedback in order to improve the performance of the joint. In a later section of this chapter it will be seen that this is not always possible to do. Thus some compromise in response may be necessary.

There is another way to reduce or eliminate the position error, however. This is accomplished by adding an integrator to the control structure. Such a scheme is referred to as PID (standing for *p*roportional, *i*ntegral, *d*erivative) control. A position servo utilizing such a controller is shown in Figure 4.3.6. In this figure the block marked "velocity loop" will usually consist of the amplifier and servomotor. In order to see how the addition of the integral term affects the final value of the joint position, we consider the following example.

EXAMPLE 4.3.2

To simplify the transient response calculations, let us assume that the inductance and viscous damping of the servomotor are zero and that the amplifier pole can be neglected (because it occurs at such a high frequency). Then the position servo of Figure 4.3.6 becomes that shown in Figure 4.3.7.

P217 Ex 4.3.2

Fig 4.3.7

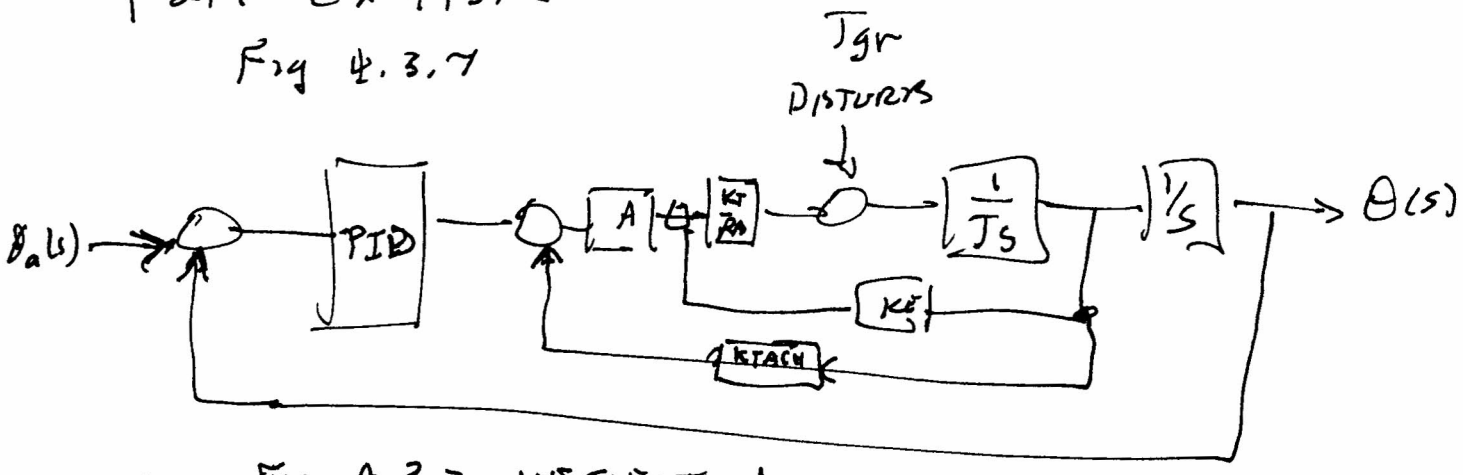

See Fig 4.3.3 NEGLECT La, B

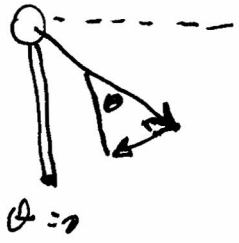

$\theta = 0$

$T_{gr} = 21 \sin\theta(t)$ oz-in

So $T_{gr}(0) = 0$

$T_{gr}(t_{final}) = 21$

CASES

I $K_P = 10/20/40$

P 220 Fig 4.3.9

POSITION ERROR

$K_P = 20$

K_D 10/0.01/0.02/0.04

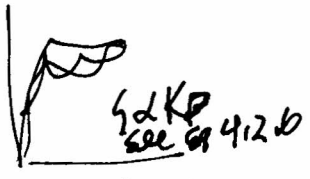

P221 F 4.3.10

POSITION ERROR

$K_D = 0.02$ NO OVERSHOOT

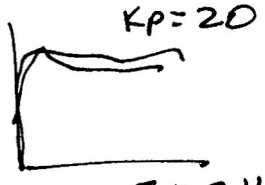

P222 F 4.3.11

K_I 2 0/75

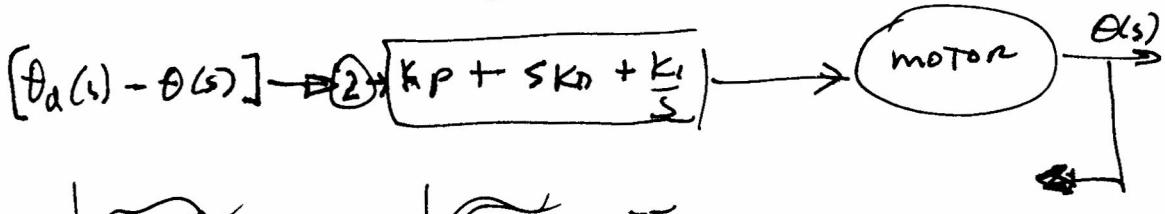

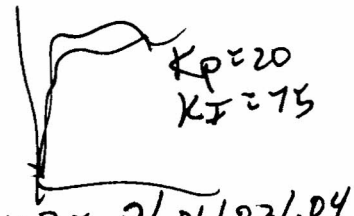

$K_D = 0/.01/02/.04$

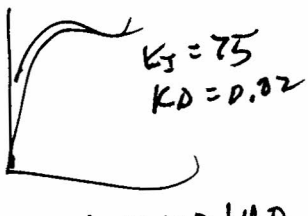

$K_P = 20/40$

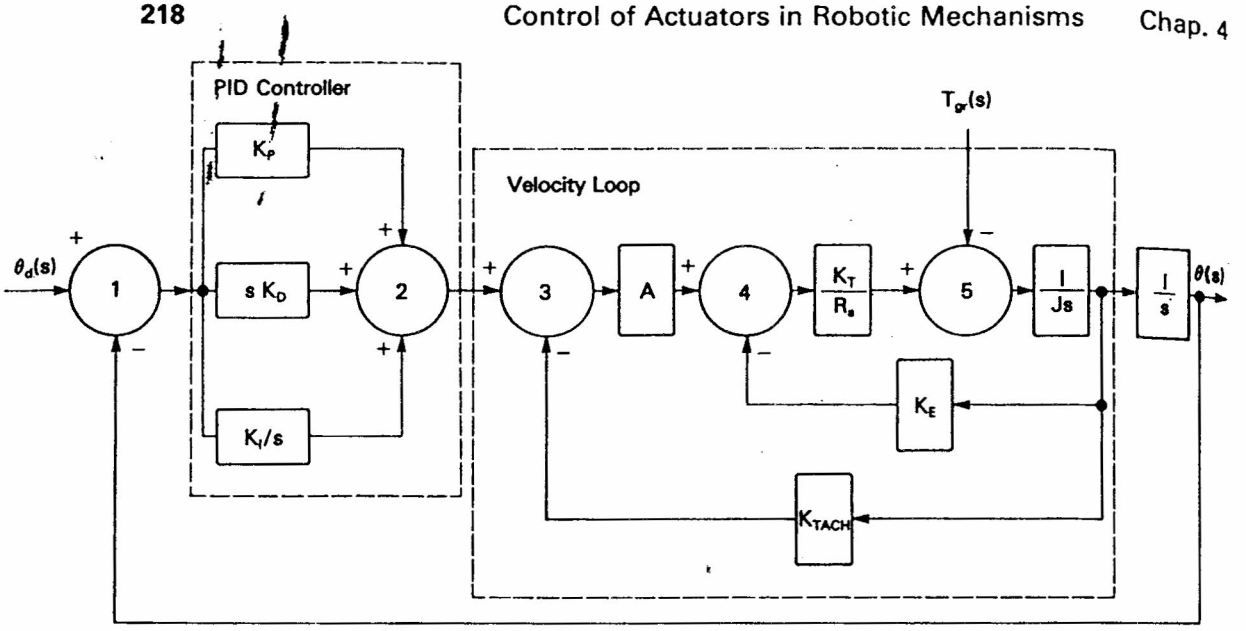

Figure 4.3.7. Position servo for Example 4.3.2.

Here summing junctions 2, 3, and 4 are assumed to be unity-voltage-gain devices (e.g., noninverting op amps). Consequently, the tachometer constant K_{tach} has the units of volts/rad/s. The specific parameters of the velocity loop are

$$A = 10.0 \text{ V/V}$$

$$R_a = 1.62\ \Omega$$

$$J_T = 0.0067 \text{ oz-in.-s}^2$$

$$K_T = 10.7 \text{ oz-in./A}$$

$$K_E = 0.0754 \text{ V/rad/s} = 7.8 \text{ V/1000 rpm}$$

$$K_{tach} = 0.056 \text{ V/rad/s} = 6 \text{ V/1000 rpm}$$

Note that J_T represents the sum of the motor and reflected load inertias. (See Section 3.3.1 for a discussion of reflected inertia calculation.)

Let the desired final position of the joint be $\pi/2$ radians, so that $\theta_d(s) = 1.57/s$. In Figure 4.3.8 it is observed that the joint is initially at $\theta = 0$ rad, so that the gravitational force produces no additional load on the axis motor. However, as θ increases with time due to the command signal, the gravitational disturbance also increases and is, in fact, proportional to the sine of θ. For a particular joint geometry, we will assume that the magnitude of this disturbance is 21 oz-in. so that the time variation of the gravitational

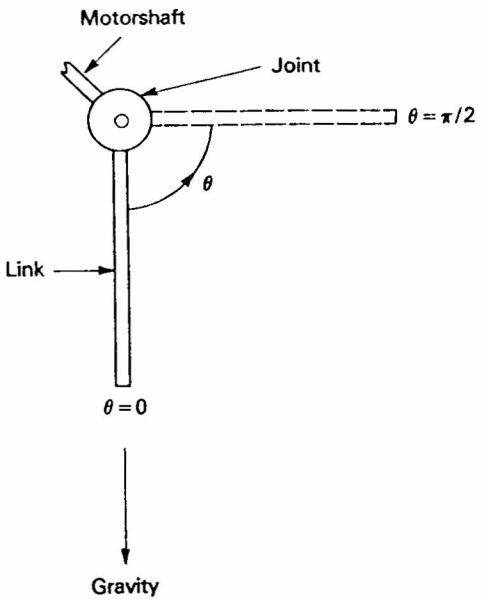

Figure 4.3.8. Joint used in Example 4.3.2. showing the effect of gravity as a function of angle.

torque will be

$$T_{gr}(t) = 21 \sin \theta(t) \tag{4.3.12}$$

The results of a computer simulation of the step response of the joint modeled in Figures 4.3.7 and 4.3.8 are given in Figures 4.3.9 through 4.3.13. The first of these figures shows the system with proportional control only. It is observed that as K_p increases, the overshoot increases, as expected. Recall the discussion in Section 4.2.2. In addition, there is also a steady-state error due to the gravitational torque disturbance. As mentioned previously, increasing K_p reduces this error but at the expense of overshoot. This is clearly demonstrated in the figure.

The effect of adding derivative control is shown in Figure 4.3.10 for a fixed proportional term (i.e., $K_p = 20$). As expected, the larger the damping (i.e., K_D), the smaller the overshoot. It is seen that it is possible to obtain a response with practically no overshoot (i.e., critical damping), but the steady-state error is still present and does not vary with K_D.

Figure 4.3.11 demonstrates the effect of adding an integral term in the controller. Here proportional plus integral (PI) control eliminates the steady-state error with slightly increased overshoot. A PID controller is used in Figure 4.3.12. In this case the step response for different values of damping is shown for $K_p = 20$ and $K_I = 75$. It is observed that it is now possible to obtain a zero steady-state error (i.e., the desired final position is actually

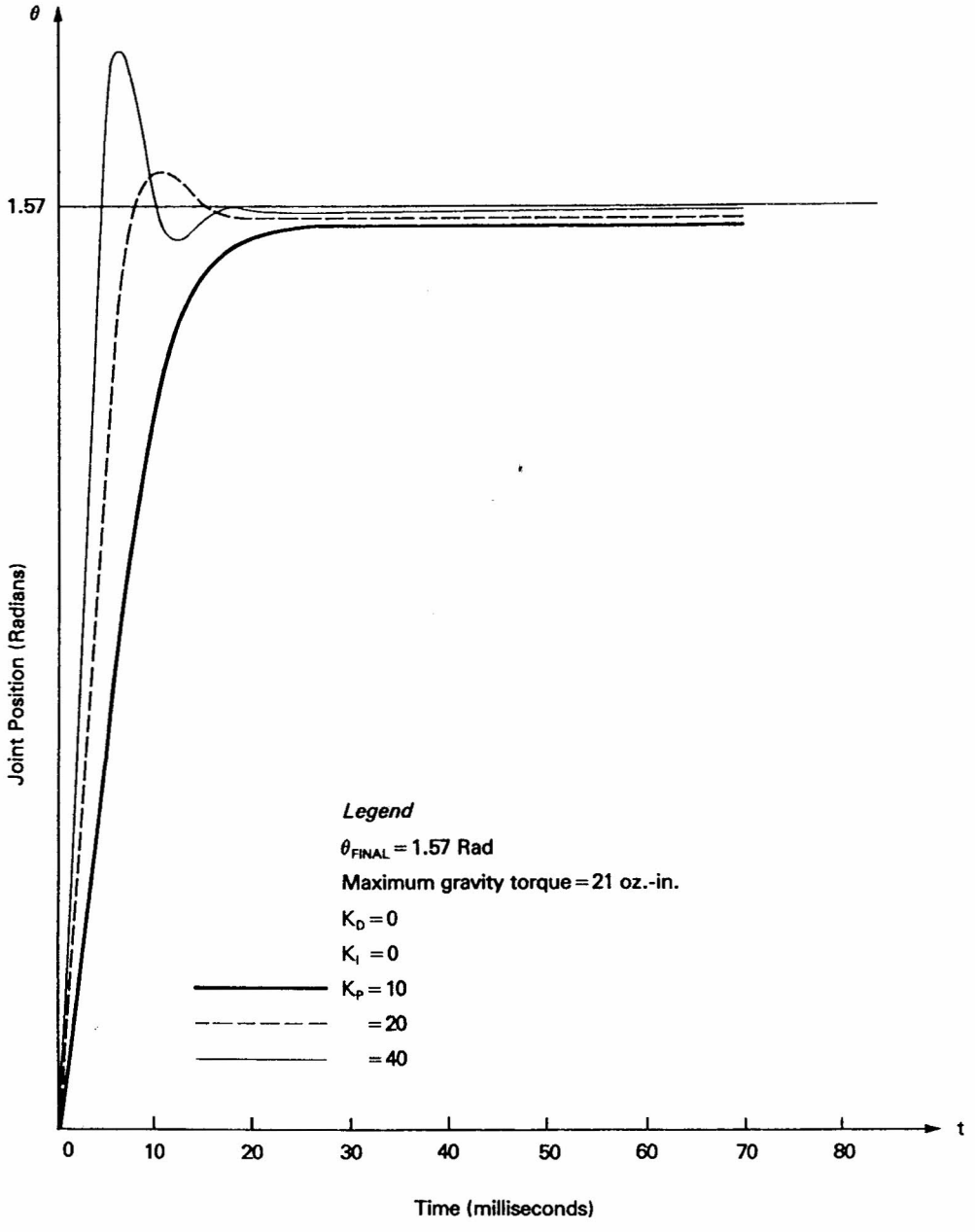

Figure 4.3.9. Step response of the system in Fig. 4.3.7 for proportional control only.

achieved) with no overshoot for $K_D = 0.02$. For completeness, a PID controller using different values of the proportional term is shown in Figure 4.3.13.

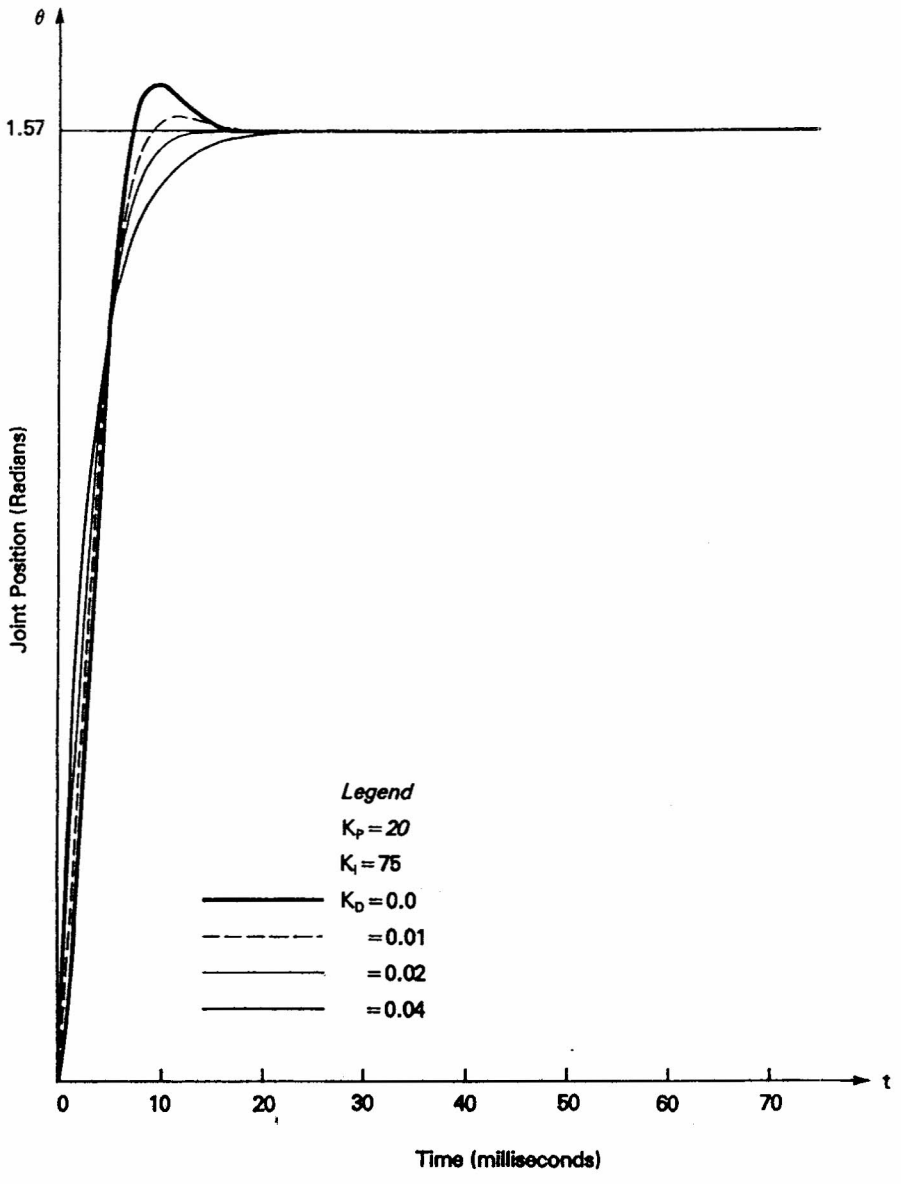

Figure 4.3.12. Step response of the system in Fig. 4.3.7 for proportional plus integral plus derivative (PID) control.

It is important to note that the PID controller can be synthesized using analog components (e.g., op amps). Alternatively, the individual joint processors can produce the required proportional, derivative, and integral terms with appropriate gain factors by operating on the error signal (see Appendix C).